SARTORIUS

Application Note

December, 2025

Keywords or phrases:
AAV8 process development, gene therapy, upstream, downstream, analytics

Addressing Challenges in Adeno-Associated Virus Manufacturing Through Innovative Process Development

Franziska Bollmann[1], Magda Tomala[1], Aishwarya Nair[2], Alexander Wood[3], Donald Traul[3], Denis Odokonyero[2], Laura Chau[2], Paul Marks[3], Pavitra Talapureddy[3], Brian Windle[3], Samantha Schrecke[2], Kevin McManus[2], Trent Lyman[2]
[1] Sartorius Stedim Biotech GmbH, August-Spindler-Straße 11, 37079 Göttingen, Germany
[2] Matica Biotechnology Inc., 2501 Earl Rudder Freeway South, 77845 College Station, TX, USA
[3] Sartorius Stedim North America Inc., 565 Johnson Avenue, 11716 Bohemia, NY, USA

Contact: franziska.bollmann@sartorius.com

Abstract

Adeno-associated virus (AAV) vectors have emerged as the predominant modality for in vivo gene therapy, facilitating long-term transgene expression and gene correction through their superior safety profile and transduction efficiency. Despite their clinical promise, scalable AAV manufacturing remains constrained by process-related bottlenecks that significantly impede commercial viability. Current AAV systems show lower volumetric productivity and greater variability than recombinant protein platforms.

This collaborative investigation between Sartorius and Matica Biotechnology employed a systematic process development approach to address critical manufacturing limitations in AAV8 vector production. The comprehensive study encompassed upstream bioprocess optimization using Ambr® 250 High Throughput bioreactor systems, followed by integrated downstream purification that incorporated harvest clarification, tangential flow filtration, chromatography, and sterile filtration operations. Through rigorous design of experiments methodologies and comparative technology assessments, we established robust operating parameters that maximized recovery, minimized impurities, and achieved reproducible enrichment of therapeutically active particles.

The integrated platform demonstrates that applying Sartorius technologies enables the development of a streamlined, industrially scalable AAV manufacturing workflow. This optimized process enhanced reproducibility, improved product quality attributes, and operational robustness, accelerating the industrial translation of AAV-based gene therapies.

For more information, visit
www.sartorius.com/en/applications/cell-and-gene-therapy/gene-therapy/aav-gene-therapy

Introduction

Clinical significance and therapeutic potential of AAV vectors

Adeno-associated virus (AAV) vectors have fundamentally transformed the landscape of in vivo gene therapy, establishing themselves as the most clinically validated and regulatory-approved delivery platform for genetic correction.[1]
The therapeutic potential of AAV systems stems from their unique biological properties: non-pathogenic nature, minimal immunogenic profile, broad tropism for both proliferating and quiescent cell populations, and capacity for sustained transgene expression in target tissues. These characteristics render AAV particularly suitable for treating chronic genetic disorders requiring long-term therapeutic intervention.

Recent clinical successes have validated the therapeutic utility of AAV vectors across diverse disease areas. Regulatory approvals for Luxturna® (for RPE65-associated Leber congenital amaurosis), Zolgensma® (for spinal muscular atrophy), and Hemgenix® (for hemophilia B) demonstrate the clinical maturity of AAV-based therapeutics. Furthermore, the robust clinical pipeline—with over 200 AAV-based investigational therapies at various phases of development—underscores the expanding therapeutic applications and commercial significance of this vector platform.

However, the broader implementation of AAV therapeutics faces substantial manufacturing constraints that limit accessibility and commercial viability. Unlike well-established recombinant protein production systems that benefit from decades of process optimization and economies of scale, AAV manufacturing remains technically challenging and economically constrained by low yields, quality inconsistencies, and limited process understanding.

Manufacturing bottlenecks and technical challenges

Contemporary AAV production faces three primary technical limitations that collectively constrain industrial scalability. First, upstream production yields remain substantially lower than those achieved in recombinant protein manufacturing. Current transient transfection-based systems utilizing HEK293 suspension cultures typically achieve viral titers of 10^{11}-10^{12} viral particles per milliliter, requiring large bioreactor volumes and extensive downstream processing to generate therapeutically relevant quantities.

Second, AAV biology inherently generates heterogeneous particle populations, including therapeutically active "full" capsids containing vector genomes and inactive "empty" capsids devoid of genetic payload. Empty particle concentrations can represent 80 - 95% of total capsid populations, significantly diluting therapeutic potency and potentially contributing to immunogenic responses. Effective separation of full and empty particles remains technically challenging and often requires sophisticated chromatographic approaches that may compromise overall process yield.
Third, the relative immaturity of AAV manufacturing platforms results in limited process understanding and control compared to established biopharmaceutical production systems. The scarcity of validated analytical methods for real-time process monitoring, combined with insufficient historical datasets for process characterization, results in high batch-to-batch variability and challenges in scaling from laboratory to commercial production.[2]

Collaborative framework and study objectives

Recognizing these fundamental challenges, Sartorius established a collaborative partnership with Matica Biotechnology to conduct comprehensive process development focused on AAV8 vector manufacturing. The strategic collaboration leveraged our extensive bioprocess technology portfolio—including high-throughput upstream systems, advanced filtration platforms, and specialized viral vector chromatography solutions—combined with Matica Biotechnology's AAV production expertise and analytical capabilities.

The study objectives were:

- Optimization of upstream production parameters using small-scale, high-throughput bioreactor systems
- Systematic evaluation of downstream unit operations for harvest clarification, concentration | buffer exchange, and chromatography
- Development of robust polishing strategies for full | empty particle separation
- Establishment of integrated workflow parameters suitable for industrial scale-up

This application note presents the outcomes of this collaborative investigation, demonstrating how systematic process development can address fundamental AAV manufacturing limitations while establishing a foundation for reproducible, commercial-scale production.

Materials

The study employed a structured, small-scale development framework encompassing upstream and downstream operations (Figure 1).

Upstream production and cell culture systems

Suspension-adapted HEK293 cells were cultured in serum-free, chemically defined medium using Ambr® 250 High Throughput bioreactor systems (Sartorius). Cell cultures were inoculated at 3.0×10^5 viable cells/mL and maintained under controlled environmental conditions: temperature 37 °C, pH ≤ 7.25 (controlled via CO_2 addition), and dissolved oxygen concentration (40% air saturation). Agitation and aeration parameters were systematically evaluated through design of experiments (DoE) methodology. Shake flask cultures served as process controls.

Transient transfection was performed 48 hours post-inoculation using the FectoVIR®-AAV transfection system (Sartorius) with previously optimized plasmid combinations. Cell harvest occurred 72 hours post-transfection via detergent-based lysis followed by nuclease digestion and clarification.

DoE for process optimization

A 2-factor full factorial DoE was implemented to evaluate the influence of agitation rate and aeration on AAV8 production. Stirrer speeds ranged from 219 to 460 rpm, while total gas flow rates varied from 2.2 to 12.8 mL/min. Statistical analysis was performed using MODDE® software (Sartorius) to identify optimal operating conditions. Process scale-up verification was conducted using Univessel® SU 2 L single-use bioreactors (Sartorius) under optimized conditions. For downstream process development, AAV8 material was produced in four Univessel® SU 2 L runs, resulting in a total of 8 L harvest. This material served as the basis for evaluating clarification, tangential flow filtration (TFF), dead-end filtration, chromatography, and final formulation steps.

Figure 1: Overview of the AAV8 production process, products evaluated, and process development activities for each step

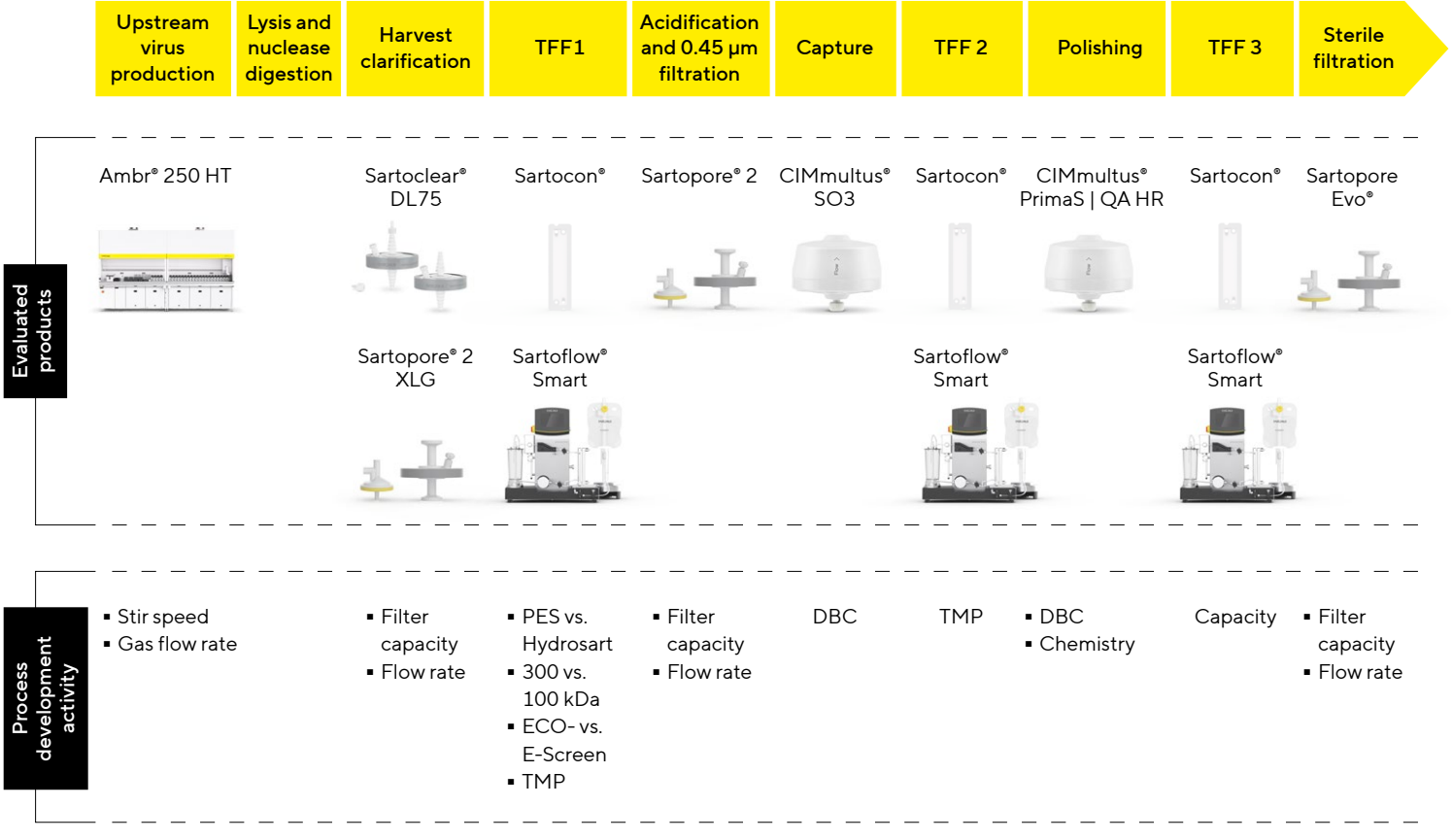

Note. DBC = dynamic binding capacity, TFF = tangential flow filtration, TMP = transmembrane pressure.

Harvest clarification and bioburden reduction

Primary clarification employed Sartoclear® DL75 depth filters (10 | 2 µm porosity gradient, capsule format, 25 cm^2 effective area; Sartorius) operated at a constant flux of 200 $L \times m^{-2} \times h^{-1}$. Filtration termination criteria included differential pressure ≥ 1.0 bar or feed exhaustion. Secondary clarification utilized Sartopore® 2 XLG filters (0.8 | 0.2 µm dual-layer design, Sartoscale 25 format, 4.5 cm^2 area; Sartorius) at 400 $L \times m^{-2} \times h^{-1}$ constant flux. Post-filtration flushing with process buffer maximized product recovery. All filtrations were performed in triplicate with comprehensive performance monitoring (weight and pressure).

Ultrafiltration | Diafiltration 1

Concentration and diafiltration operations employed the Sartoflow® Smart benchtop TFF system (Sartorius) equipped with Sartocon® Slice 200 cassettes (180 cm^2 membrane area; Sartorius). Eight cassette configurations were systematically evaluated: Hydrosart® (regenerated cellulose) and PESU (polyethersulfone) membrane chemistries, each available in 100 kDa and 300 kDa molecular weight cut-offs, combined with ECO-Screen or E-Screen cassette configurations.

Table 1: Setpoints of process parameters TMP and P1 – 3 for the first TFF step

Cassette	P1 [bar]	P2 [bar]	P3 [bar]	TMP [bar]
Hydrosart® 100 kDa ECO-Screen	1.25	0.00	0.20	0.425
Hydrosart® 300 kDa ECO-Screen	1.24	0.00	0.20	0.420
Hydrosart® 100 kDa E-Screen	1.25	0.00	0.20	0.420
Hydrosart® 300 kDa E-Screen	0.75	0.00	0.20	0.175
PESU 100 kDa ECO-Screen	1.00	0.00	0.21	0.290
PESU 300 kDa ECO-Screen	1.00	0.00	0.20	0.300
PESU 100 kDa E-Screen	1.00	0.02	0.22	0.290
PESU 300 kDa E-Screen	1.00	0.00	0.20	0.300

Transmembrane pressure (TMP) optimization involved preliminary scouting experiments to determine optimal flux-shear balance, followed by full process execution at identified setpoints (TMP, feed [P1], retentate [P2], permeate [P3]; Table 1). The concentration protocol involved 10-fold volumetric reduction followed by five diavolumes of buffer exchange into TFF1 buffer (20 mM Tris-HCl, 200 mM NaCl, 0.1% w/w Poloxamer 188, 2 mM $MgCl_2$, pH 7.5). Cassette pre-equilibration was performed with process buffer prior to viral material processing.

Due to technical constraints, the cassettes were not flushed post-processing, potentially resulting in some product loss.

Acidification and bioburden reduction

To prepare the material for capture chromatography, the concentrated feed was diluted 1:4 in capture step load buffer (50 mM sodium acetate, 50 mM NaCl, 2 mM $MgCl_2$, 0.1% Poloxamer 188, pH 4.0), lowering the pH to 4.0 without the need for additional acid addition. Samples were incubated at room temperature for 30 min to allow equilibration.

Since acidification could cause the formation of impurity aggregates, the acidified material was then filtered through pre-equilibrated Sartopore® 2 0.45 µm bioburden reduction filters (0.45 µm, Sartoscale 47 format, 17.3 cm^2 area; Sartorius). Flux rates of 50, 100, and 200 $L \times m^{-2} \times h^{-1}$ were tested. Differential pressure was monitored continuously, with 1 bar set as the cutoff. Filtration was stopped either when 1-bar differential pressure was reached or when the filtrate volume was exhausted. The filters were flushed after finishing the filtration to maximize product recovery.

Capture chromatography

Capture chromatography employed CIMmultus® SO3 monolithic columns (1 mL column volume; Sartorius) utilizing strong cation-exchange chemistry optimized for viral vector applications (a detailed protocol can be found in Nascimento et al, 2022).[3] Column equilibration was performed with loading buffer (50 mM sodium acetate, 50 mM NaCl, 2 mM $MgCl_2$, 0.1% Poloxamer 188, pH 4.0) at a flow rate of two monolith volumes per minute.

An initial capacity determination run was performed in duplicate, where acidified AAV8 feed was loaded until breakthrough was observed by UV absorbance at 280 nm. Column capacity was calculated as 7.6×10^{13} capsids/mL column volume.

Next, in duplicate process confirmation runs, 70% of the determined column capacity (5.4×10^{13} capsids/mL column volume) was loaded onto equilibrated CIMmultus® SO3 monoliths. After a wash step using the load buffer, bound vector was eluted with elution buffer (50 mM sodium acetate, 2.0 M NaCl, 2 mM $MgCl_2$, 0.1% Poloxamer 188, pH 4.0) at two monolith volumes/min. Eluted fractions were immediately neutralized with the addition of 20% (v/v) of 1 M Tris base, pH 9.0.

Ultrafiltration | Diafiltration 2

Eluate from the capture step was subjected to diafiltration into two distinct equilibration buffers tailored for subsequent polishing monoliths:

- CIMmultus® QA HR load buffer: 10 mM Bis-Tris propane, 0.1% (w/v) Poloxamer 188, 1% sucrose, 5 mM $MgCl_2$, pH 8.5
- CIMmultus PrimaS® load buffer: 10 mM Tris, 10 mM Bis-Tris propane, 0.1% (w/v) Poloxamer 188, 1% sucrose, 2 mM $MgCl_2$, pH 7.0

Diafiltration was performed on the Sartoflow® Smart TFF system using pre-equilibrated Sartocon® Slice 200 Hydrosart® 100 kDa ECO-Screen cassettes with five diavolumes exchanged. TMP scouting experiments were conducted prior to each run (Table 2), which was followed by a full process run at the identified ideal setpoints for P1 – P3 and TMP.

To improve product recovery, the cassettes were flushed twice post-processing, with the flushes being pooled with the initial retentate.

Table 2: P1 and TMP setpoints for each polishing chromatography load buffer determined through TMP scouting

Load material	P1 [bar]	TMP [bar]
CIMmultus® QA HR load	1.25	0.9
CIMmultus PrimaS® load	1.25	0.75

Polishing chromatography

Polishing chromatography utilized CIMmultus® QA HR (strong anion exchange) and CIMmultus PrimaS® (multimodal) monolithic columns for full | empty particle separation. Columns were equilibrated in their respective buffers (see Ultrafiltration | Diafiltration 2) and loaded with either 1×10^{13} or 4×10^{13} viral genomes per mL of column volume at five monolith volumes/min.

Elution was achieved using either a linear salt gradient (0 – 500 mM NaCl) for CIMmultus® QA HR or a pH gradient from 7 to 9.5 for CIMmultus PrimaS® at two monolith volumes/min. Fractions corresponding to full and empty capsids were collected separately based on UV260 and 280 profiles.

Ultrafiltration | Diafiltration 3

Fractions enriched in full capsids were pooled and concentrated to the target titer and diafiltered into the final formulation buffer (20 mM Tris, 200 mM NaCl, 1 mM $MgCl_2$, 0.005% Poloxamer 188, pH 8.0). Processing was carried out with pre-equilibrated Hydrosart® 100 kDa ECO-Screen cassettes at TMP 0.43 bar and P1 of 1.25 bar. Five diavolumes were exchanged. To improve product recovery, the cassettes were flushed twice post-processing, with the flushes being pooled with the initial retentate.

Final sterile filtration

Formulated vectors were filtered through pre-equilibrated Sartopore Evo® filters (Sartoscale 25, 4.5 cm^2 effective area). Fluxes of 50, 100, and 200 $L \times m^{-2} \times h^{-1}$ were tested. Runs were terminated either at 1 bar differential pressure or upon exhaustion of available material. Due to technical limitations, the filters were not flushed after finishing the filtrations.

Results

Analytical methods and quality assessment

To comprehensively assess process performance and product quality, a suite of analytical methods was employed throughout upstream and downstream operations.

Clarification efficiency was assessed by turbidity determination before and after filtration steps using a turbidimeter, with results expressed in nephelometric turbidity units (NTU).

Viral genome quantification employed digital droplet PCR (Bio-Rad) using AAV8-specific primer | probe sets targeting the GFP transgene sequence. Results were expressed as viral genomes per milliliter (vg/mL).

Capsid quantification utilized AAV8-specific enzyme-linked immunosorbent assays (ELISA; PROGEN Biotechnik) employing monoclonal antibodies directed against VP1 | VP2 | VP3 capsid proteins. Titers were reported as viral particles per milliliter (vp/mL).

Full-to-empty particle analysis was performed using a PATfix® biochromatography system (Sartorius BIA Separations) featuring a quaternary pump and various detectors: a multi-wavelength ultraviolet (UV) detector (190 – 700 nm, 4-channel deuterium lamp, 50 mm flow cell path length), fluorescence detector, multi-angle light scattering (MALS) detector, conductivity monitor, and pH electrode. The PATfix® analytical method was based on anion-exchange chromatography using CIMac AAV full/empty 0.1 mL Analytical Column (1.3 µm). This method enables quantitative determination of full and empty capsid populations based on peak area integration of tryptophan fluorescence, providing an accurate assessment of full particle enrichment throughout purification processes.

Host cell impurity quantification included host cell protein (HCP) analysis via ELISA (HEK293 HCP ELISA, Cygnus Technologies) and host cell DNA (hcDNA) determination using digital droplet PCR with universal primer sets. Results were expressed as ng/mL (HCP) and pg/µL (hcDNA).

Upstream process development and optimization

The Ambr® 250 High Throughput bioreactor platform demonstrated exceptional suitability for small-scale AAV8 process development, enabling systematic evaluation of critical process parameters while minimizing material consumption. Comparative analysis across the design space revealed viral titers consistently comparable to conventional shake flask controls, validating the system's ability to accurately model standard production conditions (Figure 2A). Statistical analysis of the experimental matrix identified a stirrer speed of 319 rpm combined with a gas flow rate of 7.5 mL/min as optimal, yielding maximum viral titers while maintaining favorable viral genome-to-capsid ratios indicative of efficient packaging.

Interestingly, response surface modeling indicated that the upstream process operates within a remarkably robust design space, with no individual factor demonstrating statistically significant impact on viral titer (Figure 2B). This finding suggests inherent process robustness that provides operational flexibility during scale-up and commercial manufacturing, where minor parameter deviations are inevitable. The broad operating window identified through systematic experimentation facilitates technology transfer and reduces the risk of process failures during scale-up operations.

Figure 2: Viral genome (vg) and viral capsid (vp) titer for each bioreactor of the Ambr® 250 High Throughput run **(A)**, DoE results from analysis of impact of stir speed and gas flow rate on viral capsid and genome titers **(B)**.

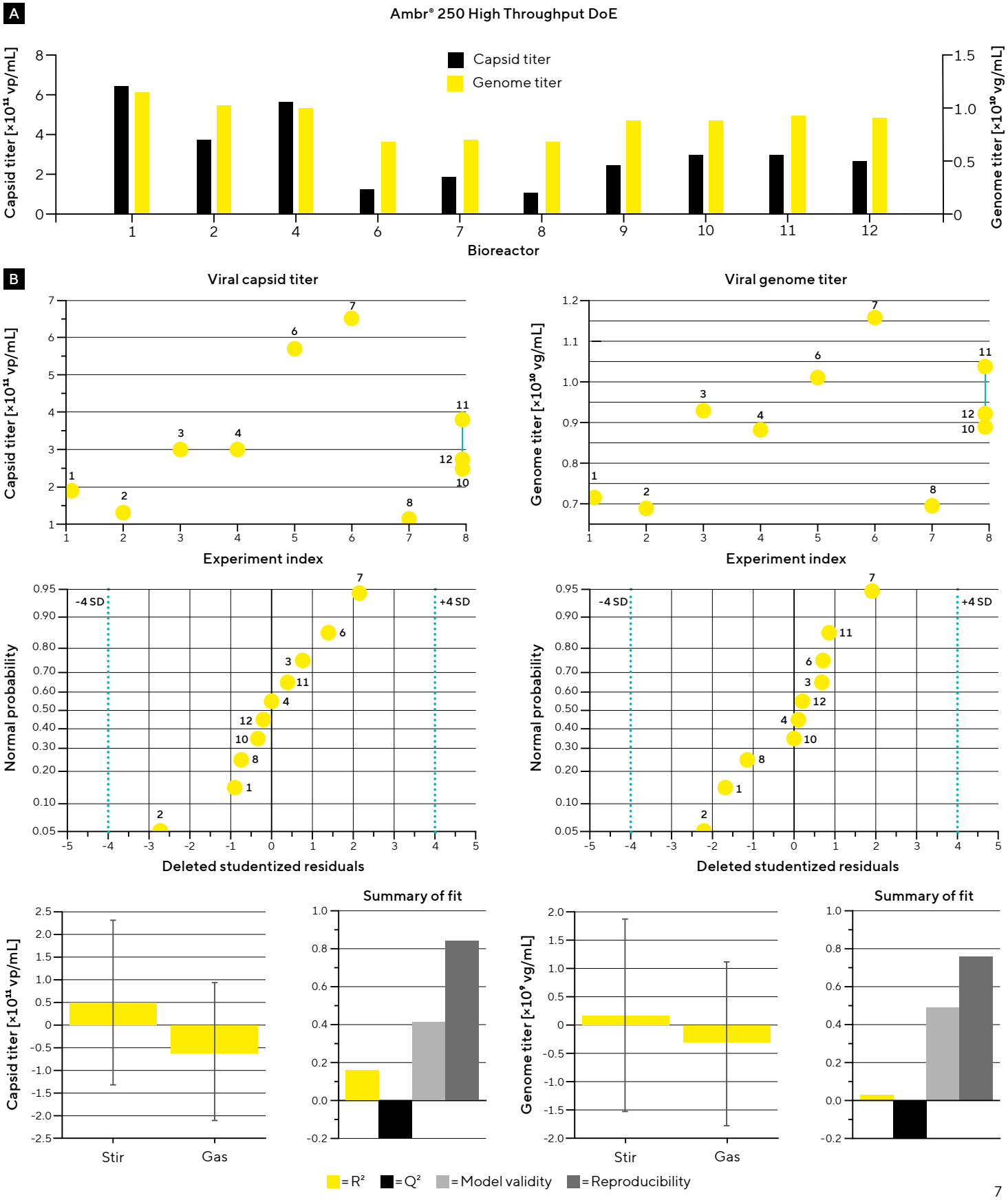

Harvest clarification performance and optimization

The two-stage clarification sequence employing Sartoclear® DL75 depth filters followed by Sartopore® 2 XLG bioburden reduction filters achieved exceptional clarification efficiency while maintaining high product recovery. Primary depth filtration demonstrated robust capacity, averaging 195 ± 18 L/m² at terminal pressure conditions (Figure 3A), while reducing turbidity from 169 NTU to 3.2 ± 1.9 NTU. The substantial turbidity reduction confirms effective removal of cellular debris and particulate matter that could compromise downstream processing efficiency.

The secondary bioburden filtration exhibited even greater robustness, with no significant pressure increase observed after processing volumes exceeding 555 L/m² (Figure 3B). This exceptional capacity indicates that the preceding depth filtration step achieved optimal clarification, minimizing the bioburden filter loading and extending operational life. Viral recovery across both filtration stages consistently exceeded 94%, demonstrating the compatibility of this filtration sequence with AAV8 processing requirements. Importantly, reproducibility was excellent, with low variability between replicate runs.

These results highlight the effectiveness of combining Sartoclear® DL75 and Sartopore® 2 XLG to achieve both clarification and bioburden reduction without compromising yield.

TFF1 performance and optimization

The first TFF step (TFF1) was designed to concentrate the viral material and remove low-molecular-weight impurities. A systematic evaluation of eight TFF cassette configurations revealed significant performance differences that affect process economics and product quality. Hydrosart® 300 kDa ECO-Screen and E-Screen and PESU 100 kDa ECO-Screen and E-Screen cassettes achieved optimal viral capsid recovery while demonstrating superior HCP clearance compared to alternative configurations (Figure 4). In contrast, PESU 300 kDa cassettes exhibited excessive permeability, resulting in substantial product loss and rendering this configuration unsuitable for AAV8 processing. The volume, flux, and pressure recordings over the process time are shown in Figure 5, demonstrating that the process parameter setpoints (TMP and P1–3) remained constant across the TFF1 runs (illustrated here using the Hydrosart® 300 kDa ECO-Screen cassette) and that there was only minimal permeate flux decay.

The superior performance of Hydrosart® membranes can be attributed to their biocompatible regenerated cellulose chemistry and optimized pore structure, which provides effective virus retention while minimizing membrane fouling and shear-induced damage. E-Screen cassettes generally demonstrated higher permeate fluxes compared to ECO-Screen configurations, although this advantage was less pronounced for Hydrosart® membranes, suggesting membrane chemistry plays a more critical role than cassette configuration in AAV8 applications.

Figure 3: Pressure monitored across filtrate weight for the harvest clarification using **(A)** Sartoclear® DL75 in capsule format followed by **(B)** Sartopore® 2 XLG in Sartoscale 25 format

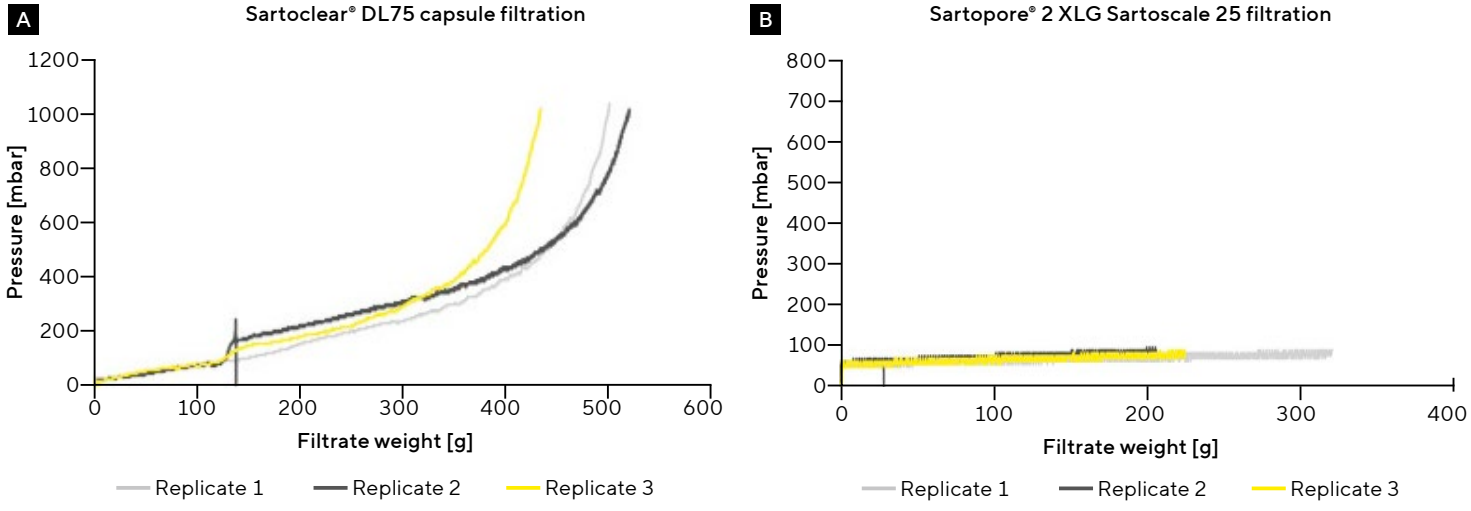

Figure 4: Comparison of the performance of all TFF cassettes

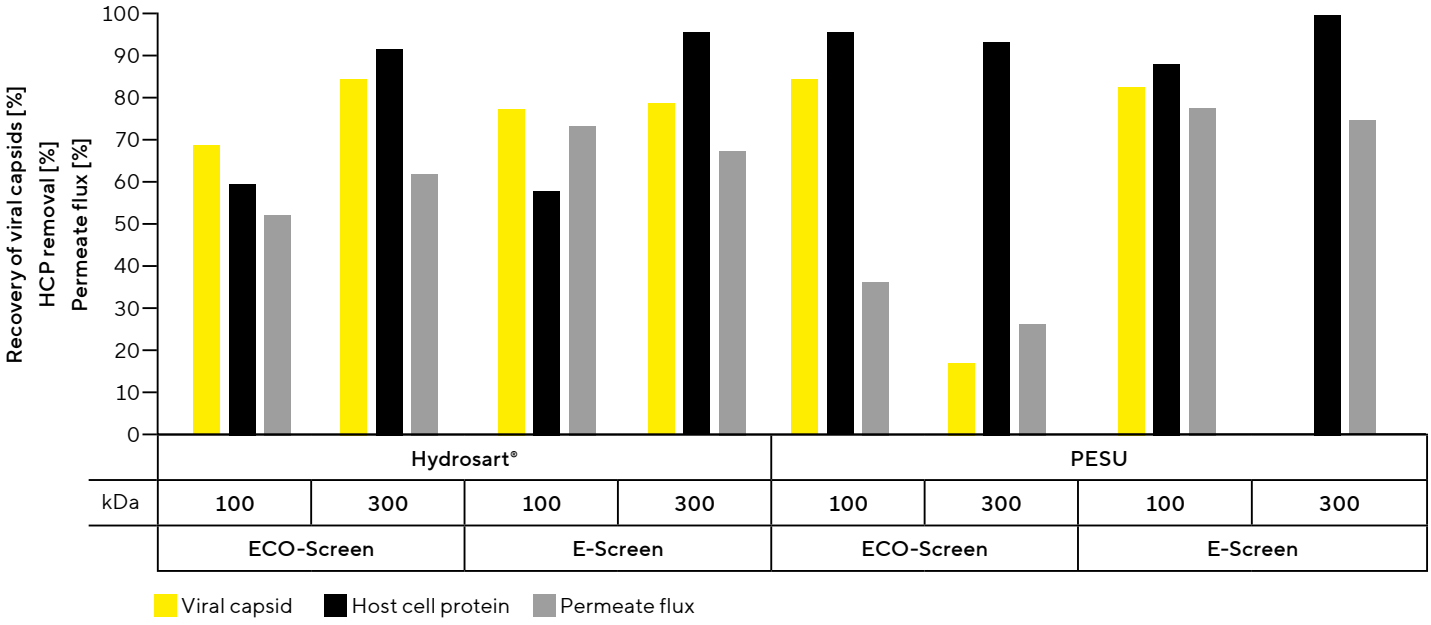

Note. Viral particle recovery only refers to the retentate; no flush was collected.

Figure 5: Recordings of process parameters during TFF1 using Hydrosart® 300 kDa ECO-Screen. Retentate volume, permeate volume, and permeate flux over process time **(A)**, and permeate flux and pressure over process time **(B)**

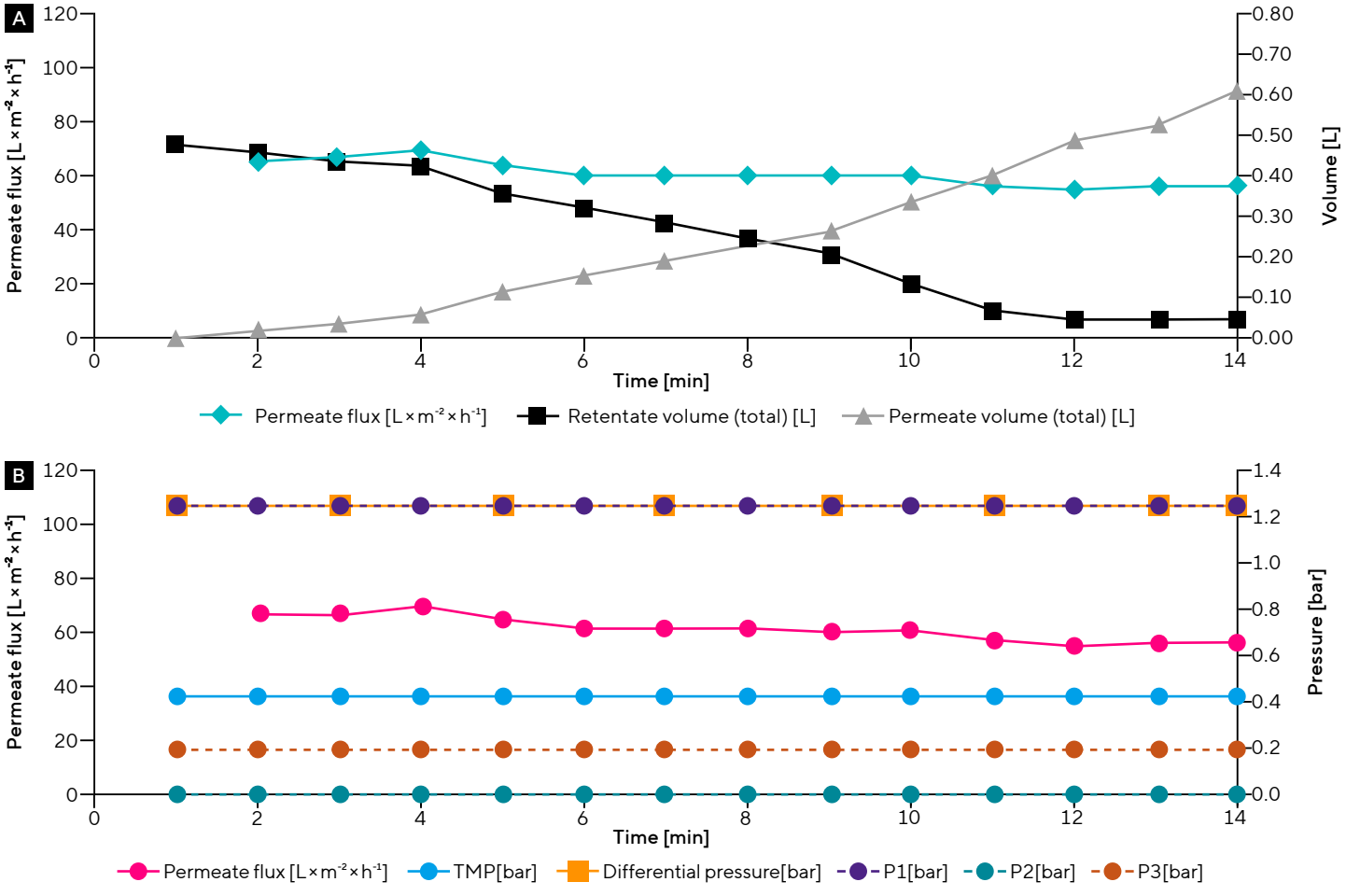

Acidification and bioburden reduction performance and optimization

Following primary concentration via TFF1, the AAV8 material required pH adjustment to facilitate optimal binding during subsequent cation-exchange capture chromatography. This critical conditioning step was accomplished through controlled dilution (1 : 4 volumetric ratio) in a specifically formulated load buffer, achieving the target pH of 4.0 without exogenous acid addition. A 30-minute equilibration period at ambient temperature ensured complete pH homogenization throughout the viral suspension while minimizing potential aggregation kinetics.

Given the propensity for protein aggregation and particulate formation under acidic conditions, immediate bioburden reduction was implemented using Sartopore® 2 0.45 µm membrane filters (Sartoscale 47 format, 17.3 cm^2 effective area). Systematic flux evaluation at 50, 100, and 200 $L \times m^{-2} \times h^{-1}$. revealed exceptional filtration performance across all tested conditions. Notably, differential pressure remained stable throughout processing, remaining below the 1.0 bar operational limit, indicating substantially higher true filter capacity than the processed volumes (Table 3). Due to limited feed material availability, the maximum filter capacity per flux rate could not be determined; therefore, no differences could be detected.

Quantitative assessment of filtration efficiency demonstrated robust clarification performance, with feedstock turbidity consistently reduced to 4-5 NTU post-filtration (Table 3). This turbidity reduction confirms effective removal of acid-induced aggregates and particulate matter that could compromise downstream chromatographic performance.

Table 3: Filter performance in bioburden filtration after acidification using Sartopore® 2 0.45 µm

Flux rate [$L \times m^{-2} \times h^{-1}$]	200	100	50
Processed volume [L]	202.1	103.2	49.1
Filter capacity [L/m^2]	> 117	> 60	> 28
Final turbidity [NTU]	4.4	4.7	5.0

Viral recovery analysis revealed exceptional product retention, with both genome and capsid titers maintained at near-quantitative levels (≥89% recovery) across all flux conditions (Figure 6). A marginal trend toward enhanced recovery at lower flux rates was observed, likely reflecting reduced shear stress from the pump, or reduced inertial impaction within the filter, though the magnitude of this effect was not statistically significant.

Figure 6: AAV8 recovery from bioburden filtration after acidification using Sartopore® 2 0.45 µm

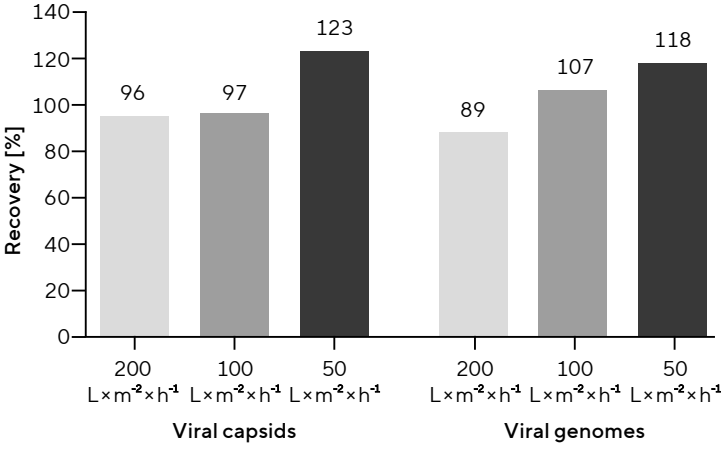

The integrated acidification and bioburden reduction sequence demonstrated exceptional process robustness, delivering appropriately conditioned material with optimal pH and clarity for subsequent capture chromatography.

Capture chromatography performance

The capture step employed CIMmultus® SO3 monoliths, which leverage cation-exchange chemistry tailored to viral vectors. Breakthrough experiments established a binding capacity of approximately 7.6×10^{13} capsids per mL of monolith volume (performed in duplicate). Based on this value, operational loading was set at 70% of capacity to avoid premature breakthrough during preparative runs. Under these conditions, duplicate confirmation experiments yielded an average viral capsid recovery of 72% ± 6%, accompanied by a 79% ± 2% (0.67 $\log_{10}$) reduction in HCP content. Chromatographic profiles exhibited sharp and symmetrical elution peaks, indicating robust and reproducible binding and release (Figure 7).

These findings confirm the effectiveness of CIMmultus® SO3 for capturing AAV8 from clarified harvests, providing both concentration and impurity reduction in a single step.

Figure 7: Chromatograms of two AAV8 capture chromatography runs using CIMmultus® SO3

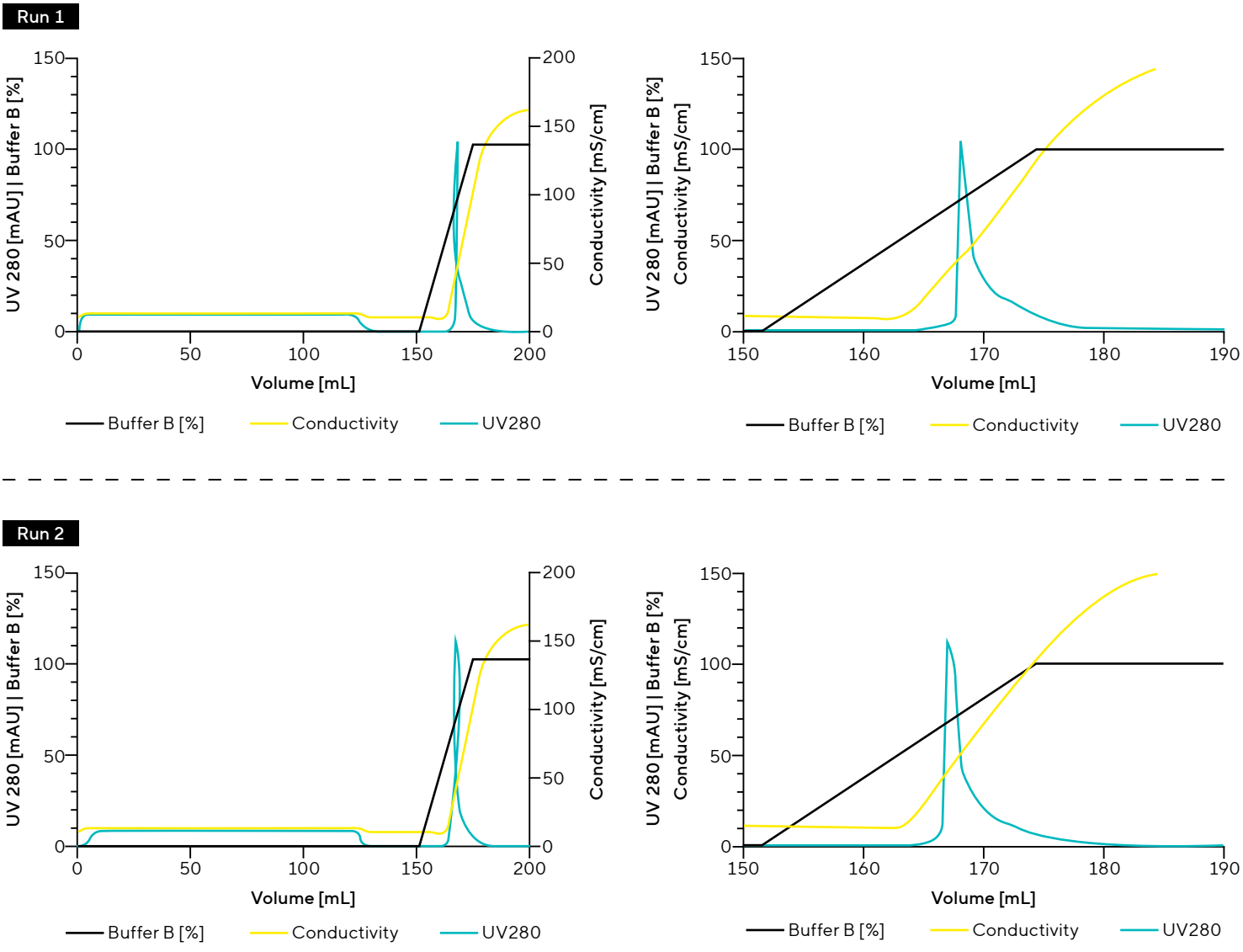

TFF2 performance and optimization

A second TFF step (TFF2) was required to exchange the capture elution buffer into one suitable for polishing chromatography. Again, stable flux profiles were achieved. Subsequent bioburden reduction filtration using Sartopore® 2 0.45 µm filters exhibited excellent filtration performance with filter capacities exceeding 600 L/m². Viral recovery across both unit operations was robust, with genome and capsid titers maintained at high levels (i.e., ~80%), confirming the suitability of the selected cassette for formulation into chromatography-compatible buffers.

Polishing chromatography performance

The comparison of polishing chromatography between CIMmultus® QA HR and CIMmultus PrimaS® revealed the ability of both columns to resolve distinct peaks corresponding to empty and full particles (Figure 8), but performance varied in terms of recovery and full particle enrichment.

The CIMmultus® QA HR monolith provided robust separation at both tested loading densities, yielding enriched fractions of full capsids with high reproducibility. However, CIMmultus PrimaS® outperformed CIMmultus® QA HR, achieving enrichment of full capsids from 18% in the post-capture material to 82% in the polished product as determined by PATfix® analysis.

This represents a 4.5-fold enrichment, whereas CIMmultus® QA HR achieved an enrichment of 3.6-fold (Figure 9). Viral genome recovery reached 121%, while capsid recovery in the full fraction remained limited to 28%, reflecting efficient removal of empty particles. Viral genome recovery in the full elution fractions of CIMmultus® QA HR was 100% and viral particle recovery 32%, similar to recoveries achieved with CIMmultus PrimaS®.

Taken together, these results indicate that CIMmultus PrimaS® monolith delivers the most effective polishing performance for AAV8, enabling both high recovery of genome-containing particles and substantial enrichment of the therapeutically active fraction.

Figure 8: Chromatogram showing the separation of full and empty AAV8 capsids using CIMmultus® QA HR and PrimaS®, with a zoom-in on the full and empty peak fractions during the elution phase.

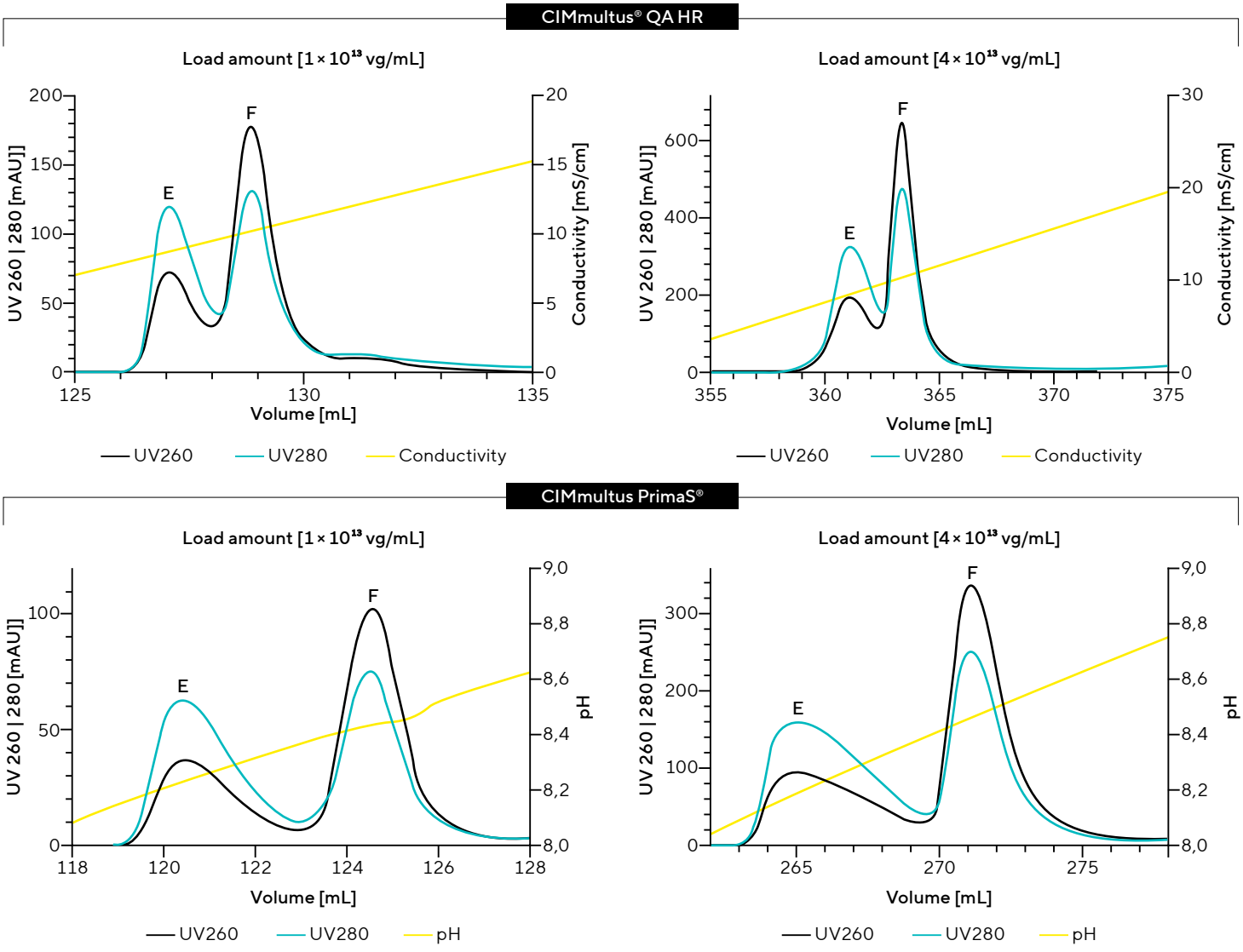

Note. E = empty particles peak, F = full particles peak

Performance and optimization of final formulation and sterile filtration

Following polishing, the product was subjected to a third TFF step (TFF3) for concentration to the desired titer, relevant for diafiltration into the final formulation buffer and therapeutic application. The Hydrosart® 100 kDa ECO-Screen cassette provided excellent performance, achieving 97% viral genome recovery and 90% capsid recovery. Permeate flux (~93 L × m^{-2} × h^{-1} remained stable throughout the process, confirming the robustness of the selected operating conditions.

Sterile filtration was conducted using Sartopore Evo® filters, which employ a PES membrane as an alternative to conventional sterilizing-grade PVDF membranes. This filtration technology aligns with increasing regulatory focus on sustainable manufacturing practices.

Evaluation across multiple flux rates revealed consistently high viral recovery, with capsid recoveries exceeding 81%. Due to technical limitations, the filters were not flushed after the filtrations were completed, which likely explains the somewhat reduced product recovery at this step.

However, no significant increase in differential pressure was observed during the runs, indicating high filter capacity and minimal fouling. These findings demonstrate that Sartopore Evo® provides both environmental and operational advantages, ensuring product safety without sacrificing yield.

Process integration and overall performance assessment

The integrated workflow demonstrated excellent process robustness and product quality attributes suitable for clinical and commercial applications.

The comprehensive process described here could potentially achieve overall viral genome recovery between 30 and 40%, with a significant reduction in HCP and hcDNA. Furthermore, the substantial enrichment of full particles (> 4-fold) significantly enhances therapeutic potency while potentially reducing immunogenic burden associated with empty capsid administration.

Figure 9: AAV8 capsid recovery **(A)**, genome recovery **(B)**, and full particle enrichment **(C)** following polishing chromatography with CIMmultus® QA HR and CIMmultus PrimaS®.

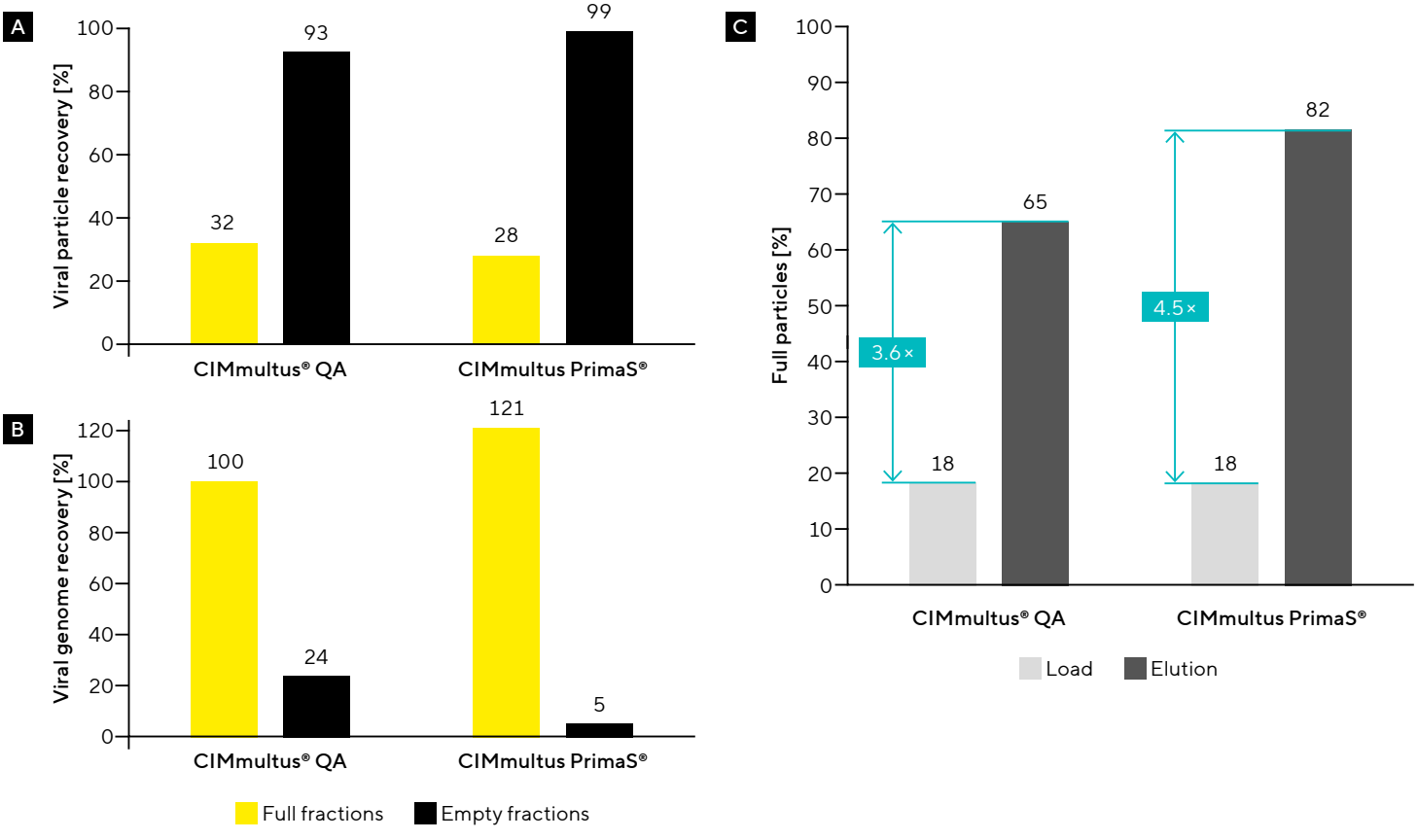

Note. Analytical results from combined fractions of 1×10^{13} and 4×10^{13} vg/mL load runs

Conclusion

This collaborative investigation demonstrates that systematic process development combining advanced bioprocess technologies can effectively address the fundamental limitations constraining the scalability of AAV manufacturing. The integrated platform established during this study provides a robust foundation for commercial AAV8 production, offering enhanced yields, improved product quality, and operational flexibility essential for industrial implementation.

The upstream studies confirmed that the Ambr® 250 High Throughput bioreactor is a robust platform for defining operating ranges for AAV8 production. It enabled the reliable identification of agitation and aeration conditions that could be transferred to larger scales without compromising performance. The clarification sequence—combining Sartoclear® DL75 depth filtration with Sartopore® 2 XLG sterile filtration—proved highly effective, consistently yielding clarified material of low turbidity while maintaining high recovery. This strategy provided reproducible performance across multiple runs.

In the downstream phase, small-scale Sartocon® Slice cassettes operated on the Sartoflow® Smart system enabled rapid screening of TFF conditions with minimal AAV material. This approach enabled the direct comparison of membrane materials, cut-offs, and cassette configurations, revealing distinct differences in process flux, product recovery, and impurity removal. The clear contrasts observed provided a strong basis for selecting the most suitable cassette, allowing the TFF step to be optimized quickly and efficiently.

Capture chromatography with CIMmultus® SO3 ensured robust viral recovery and impurity clearance, while polishing with CIMmultus PrimaS® provided superior separation of empty and full capsids, achieving up to 4.5-fold enrichment of therapeutically active particles. Finally, final formulation and sterile filtration confirmed that high product recovery can be maintained through the last stages of processing.

The workflow's scalability is facilitated by the use of established unit operations and commercially available equipment platforms, enabling straightforward technology transfer from development to manufacturing scales. Furthermore, the process robustness demonstrated across multiple unit operations provides confidence in the system's ability to maintain consistent performance under commercial manufacturing conditions.

These findings contribute to the broader effort to democratize access to gene therapy by reducing manufacturing barriers that have historically limited the commercial viability of AAV-based therapeutics. By enabling more efficient and cost-effective production, this integrated approach directly supports the expansion of gene therapy applications to larger patient populations.

References

1. Wang, D., Tai, P. W. L., & Gao, G. (2019). Adeno-associated virus vector as a platform for gene therapy delivery. *Nature Reviews Drug Discovery,* 18(5), 358–378. https://doi.org/10.1038/s41573-019-0012-9

2. Wright, J. F. (2008). Manufacturing and characterizing AAV-based vectors for use in clinical studies. *Gene Therapy,* 15(11), 840–848. https://doi.org/10.1038/gt.2008.65

3. Nascimento, A., Faria, T. Q., Bollmann, F., Noverraz, M., Pressac, G., Roldão, A., Peixoto, C., & Silva, R. J. S. (2025). Purification of AAV8 through a scalable two-step monolithic chromatography approach. *Journal of Chromatography A,* 1740, 465586. https://doi.org/10.1016/j.chroma.2024.465586

Germany
Sartorius Stedim Biotech GmbH
August-Spindler-Strasse 11
37079 Göttingen
Phone +49 551 308 0

USA
Sartorius Stedim North America Inc.
565 Johnson Avenue
Bohemia, NY 11716
Toll-Free +1 800 368 7178

For more information, visit
sartorius.com

Last modified: 01 | 2026